and co-workers (K_{eq} = 8.93) under very similar conditions (46 °C; toluene solution), but values of $k_9 + k_{-9}$ for the two studies are in reasonable agreement (2.28 (3) × 10^{-4} s^{-1} at 44.5 °C (this study) vs 3.5 (4) × 10^{-4} s^{-1} (Howell et al.[12])). No reason for the lack of agreement for K_{eq} is apparent. The highly positive entropies of activation for both isomerization processes ($\Delta S_9^{\ddagger}$ = 22.4 (14) cal/(deg mol) and $\Delta S_{-9}^{\ddagger}$ = 21.6 (16) cal/(deg mol)) are consistent with significantly greater organization in the ground states than the transition state, but there is no evidence to support dissociation of P(*n*-Bu)$_3$ during the isomerization process.

Summary. The overall mechanism favored by the evidence presented here for displacement of DTHp by L from (DTHp)W(CO)$_4$, together with values of the rate constants for individual reaction steps as determined at 35.2 °C in CB, are given in eq 18.

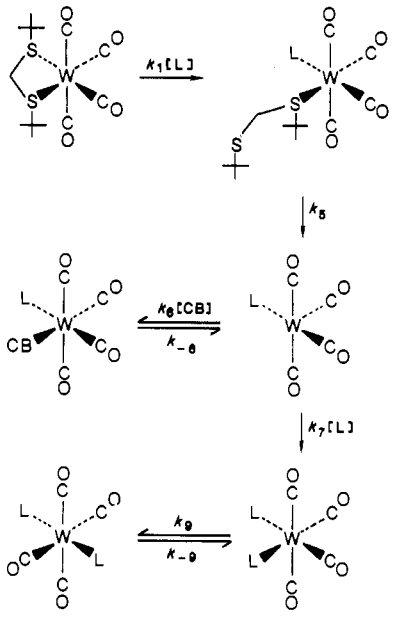

(18)

CB = chlorobenzene; L = P(O-*i*-Pr)$_3$

k_1 = 2.61 (5) × 10^{-2} M^{-1} s^{-1}

k_5 = 3.27 (1) × 10^{-4} s^{-1}

k_5 = 3.27 (1) × 10^{-4} s^{-1}

k_9 = 3.56 × 10^{-5} s^{-1} (35.5 °C)

k_{-9} = 1.21 × 10^{-5} s^{-1} (35.5 °C)

k_7/k_6 = 1.14 (20)

Acknowledgment. The support of this research by the National Science Foundation (Grant No. CHE 84-15153) is gratefully acknowledged. The flash photolysis experiments and analyses of the data produced were carried out at the Center for Fast Kinetics Research (CFKR), University of Texas at Austin. The CFKR is supported jointly by the Biotechnology Branch of the Division of Research Resources of the NIH (Grant No. RR00886) and by the University of Texas at Austin. The help and expertise of the staff at CFKR are greatly appreciated. We also appreciate the experimental assistance of T. Corby Young, David Dumond, and Hani H. Awad.

Supplementary Material Available: Values of k_{obsd} for the thermal reaction of *cis*-(DTHp)W(CO)$_4$ with L to afford *cis*-(L)(η^1-DTHp)W(CO)$_4$ and for the further reaction of this intermediate with L to afford *cis*-(L)$_2$W(CO)$_4$ (Supplementary Tables I and II, respectively), rate constants at various temperatures for unimolecular ring closure in *cis*-[(solv)(η^1-DTHp)W(CO)$_4$] complexes after flash photolysis (solv = 1,2-dichloroethane, bromobenzene) (Supplementary Table III), pseudo-first-order rate constants for thermal reactions of P(O-*i*-Pr)$_3$ with *cis*-[(CB)(P(O-*i*-Pr)$_3$)W(CO)$_4$] produced after flash photolysis of *cis*-(pip)(P(O-*i*-Pr)$_3$)W(CO)$_4$ at 35.2 °C (Supplementary Table IV), and pseudo-first-order rate constants and values of K_{eq} for the cis-trans isomerization of *cis*-(P(*n*-Bu)$_3$)$_2$W(CO)$_4$ (Supplementary Table V) (7 pages). Ordering information is given on any current masthead page.

Contribution from the Center for Organometallic Research and Department of Chemistry, University of North Texas, Denton, Texas 76203-5068

Octahedral Metal Carbonyls. 64.[1] Ligand Exchange in *fac*-(py)(diphos)Mo(CO)$_3$ in Toluene (T) Solution (Py = Pyridine; Diphos = 1,2-Bis(diphenylphosphino)ethane): The *fac*-[(T)(diphos)Mo(CO)$_3$] Intermediate

Khalil J. Asali,[2] Gideon J. van Zyl,[3] and Gerard R. Dobson*

Received March 14, 1988

fac-(py)(diphos)Mo(CO)$_3$ (**1**; py = pyridine; diphos = 1,2-bis(diphenylphosphino)ethane) reacts thermally with phosphines, phosphites, and triphenylstibine (=L) in toluene to afford *fac*-(L)(diphos)Mo(CO)$_3$ products (**2**). The observed rate law suggests that the mechanism involves dissociation of py from **1** and competitive reaction of the resulting steady-state intermediate, *fac*-[(diphos)Mo(CO)$_3$] (**3**), with py (reversibly) and with L (irreversibly). Pulsed laser flash photolysis of (diphos)Mo(CO)$_4$ also affords **3**, identified through comparisons of its reactivities with L to those observed for **3** produced thermally. Evidence suggests, however, that a *predominant reaction species* formed after pulsed laser flash photolysis of (diphos)Mo(CO)$_4$ is *fac*-[(T)(diphos)Mo(CO)$_3$] (**4b**) (T = toluene), in which toluene occupies a site in the octahedral coordination sphere of Mo and probably interacts with Mo via an "agostic" hydrogen; reversible dissociation of toluene from **4b** affords **3**. Rate data after flash photolysis also support the formation of [(η^1-diphos)Mo(CO)$_4$] and *cis*-[(T)(η^1-diphos)Mo(CO)$_4$] (**5**). The latter undergoes irreversible chelate ring closure with concerted expulsion of toluene to afford (diphos)Mo(CO)$_4$. Rate constants and activation parameters for various reaction steps are presented and are discussed in terms of the steric and electronic properties of L.

Introduction

Recent studies have demonstrated that intermediates produced upon flash photolysis of group VIB metal carbonyl derivatives can be identified through their kinetics behavior even where spectroscopic methods are inadequate for the task.[4-6] Thus, for example, where photolysis induces chelate ring opening in (η^2-chelate)M(CO)$_4$ complexes (M = Cr, Mo, W) to afford solvated *cis*-[(η^1-bidentate)M(CO)$_4$] species, the latter can be identified on the basis of the two-term rate law expected and observed for

(1) Part 63: Dobson, G. R.; Cortes, J. E. *Inorg. Chem.*, preceding paper in this issue.
(2) Present address: Department of Chemistry, College of Education, King Saud University, Abha Branch, Abha, Saudi Arabia.
(3) Present address: Department of Chemistry, University of the Orange Free State, Bloemfontein, Republic of South Africa.
(4) Dobson, G. R.; Bernal, I.; Reisner, G. M.; Dobson, C. B.; Mansour, S. E. *J. Am. Chem. Soc.* **1985**, *107*, 525.
(5) Dobson, G. R.; Dobson, C. B.; Mansour, S. E. *Inorg. Chem.* **1985**, *24*, 2179.
(6) Asali, K. J.; Basson, S. S.; Tucker, J. S.; Hester, B. C.; Cortes, J. E.; Awad, H. H.; Dobson, G. R. *J. Am. Chem. Soc.* **1987**, *109*, 5386.

0020-1669/88/1327-3314$01.50/0

Table I. Analytical Data for *fac*-(L)(diphos)Mo(CO)$_3$ Complexes[a]

L	ν(CO), cm^{-1}			anal. % calcd		anal. % found	
	A′	A′	A″	C	H	C	H
C_5H_5N	1942 (vs)	1857 (s)	1839 (s)				
$P(OCH_2)_3CCH_3$	1959 (vs)	1881 (s)	1866 (vs)	56.21	4.58	56.03	4.52
$P(OMe)_3$	1959 (vs)	1881 (s)	1865 (vs)	54.79	4.60	55.23	4.84
$P(OEt)_3$	1958 (vs)	1880 (s)	1865 (vs)	56.46	5.28	56.53	5.21
$P(O\text{-}i\text{-}Pr)_3$	1957 (vs)	1877 (s)	1859 (s)				
PPh_3	1954 (vs)	1869 (s)	1845 (s)	67.15	4.68	67.03	4.85
P(*o*-tol)Ph$_2$	1953 (vs)	1860 (s)	1844 (s)	67.45	4.83	67.59	5.10
P(*o*-tol)$_2$Ph			1844				
$SbPh_3$	1954 (vs)	1872 (s)	1869 (s)				

[a] Cyclohexane solution, except for P(*o*-tol)$_2$Ph, whose spectrum was recorded in 1,2-dichloroethane.

their decay, via unimolecular chelate ring closure and bimolecular interaction of the intermediate with an incoming nucleophile, L, usually an alkyl or aryl phosphite or an alkyl- or arylphosphine.[4,5] Comparisons of these data with thermal rate data for reactions in which it is presumed that such *cis*-[(η^1-bidentate)M(CO)$_4$] species are steady-state intermediates also confirm their identities.

In thermal ligand-substitution reactions of group VIB complexes containng *mono*dentate ligands, e.g., *cis*-(pip)(L′)W(CO)$_4$ (pip = piperidine), intermediates such as *cis*-[(solvent)(L′)W(CO)$_4$] can also be identified through investigations of their reactivities with L or olefins where pulsed laser flash photolysis provides access to them within thermal ligand-substitution pathways. These intermediates may be produced in greater variety and are of general interest through their roles as models for species implicated in a number of important homogeneous catalytic processes.[7]

These methods may be applied to thermal ligand-exchange reactions through which other types of postulated steady-state intermediates can be evaluated. Herein are reported parallel thermal and pulsed laser flash photolysis investigations of the ligand-exchange reactions of *fac*-(py)(diphos)Mo(CO)$_3$ (**1**; diphos = 1,2-bis(diphenylphosphino)ethane, py = pyridine) with L in toluene to afford *fac*-(L)(diphos)Mo(CO)$_3$ complexes; access into the thermal ligand-exchange process is effected through flash photolysis of (diphos)Mo(CO)$_4$.

Experimental Section

General Information. Infrared spectra were obtained by employing a Perkin-Elmer 1710 FTIR spectrometer. Chemical analyses were carried out by Midwest Microlab, Indianapolis, IN.

Materials and Syntheses. Pyridine (Fisher) was fractionally distilled under N_2 from KOH. The ligands $P(OMe)_3$, $P(OEt)_3$, and $P(O\text{-}i\text{-}Pr)_3$ were fractionally distilled under reduced pressure (0.1–0.2 Torr) from sodium by using a nitrogen bleed. 4-Methyl-2,6,7-trioxa-1-phosphabicyclo[2.2.2]octane, $P(OCH_2)_3CCH_3$ (CP), was prepared according to the literature method[8] and was then twice vacuum-sublimed into a wide-mouthed condenser (70 °C, 0.1 Torr). Triphenylphosphine (Fluka) and triphenylstibine (Aldrich) were recrystallized from absolute ethanol and were then dried under vacuum. The ligands PPh_2(*o*-tol), PPh(*o*-tol)$_2$, and P(*o*-tol)$_3$ (*o*-tol = *o*-tolyl) (Strem) were used as obtained.

Toluene (Fisher) was fractionally distilled over P_4O_{10} (nitrogen bleed), while tetrahydrofuran (THF; Fisher) was distilled from $LiAlH_4$ under nitrogen. Cyclohexane and hexanes (Fisher) and $Mo(CO)_6$ (Climax) were used as obtained.

Diphos and (diphos)Mo(CO)$_4$ were synthesized and purified through use of the literature method.[9]

***fac*-(py)(diphos)Mo(CO)$_3$.** The following synthesis is more convenient than the literature preparation.[10] (diphos)Mo(CO)$_4$ (4.3 g; 7.1 mmol) was dissolved in 200 mL of dry THF, and the solution was irradiated under N_2 in a quartz immersion reactor for 1 h with a 450-W Hanovia medium-pressure Hg lamp. Excess py (10 mL) was added to the solution, which was then stirred for 30 min. Solvent and excess py were completely removed under vacuum, and the solid residue was dissolved in 40 mL of warm (35 °C) toluene containing 3 mL of py. This solution was filtered by suction under nitrogen into 80 mL of cold (0 °C) hexanes, and the solution was allowed to stand overnight in a freezer. The bright yellow product (3.8 g, 82% yield) was collected by suction filtration and was dried under vacuum. Its carbonyl stretching spectrum, in good agreement with the literature spectrum, which was recorded in $CHCl_3$,[10] is given in Table I.

***fac*-(CP)(diphos)Mo(CO)$_3$.** A 0.10-g amount of *fac*-(py)(diphos)-Mo(CO)$_3$ (0.15 mmol) and 30 mg of CP (0.2 mmol) in 10 mL of toluene were heated with stirring under nitrogen at 45 °C for 1 h. After this time, the yellow solution had become colorless. It was filtered warm under nitrogen, and 20 mL of hexanes was added. Colorless crystals precipitated upon cooling overnight in a freezer. They were collected by suction filtration, washed several times with hexanes, and dried under vacuum. This method was also employed to prepare the analogous complexes for L = $P(OMe)_3$, $P(OEt)_3$, $P(OPh)_3$, $P(O\text{-}i\text{-}Pr)_3$, PPh_3, $SbPh_3$, and PPh_2(*o*-tol). Carbonyl stretching frequencies for all of these complexes and elemental analyses for representative complexes are presented in Table I.

Since this ligand-exchange reaction was being studied photochemically as well as thermally, *fac*-(PPh_3)(diphos)Mo(CO)$_3$ was also synthesized via a photochemical pathway analogous to that employed for synthesis of *fac*-(py)(diphos)Mo(CO)$_3$.

Thermal Kinetics Studies. Thermal kinetics runs were carried out in sealed 10-mm Pyrex screw-capped cells (Spectrocell) maintained at constant temperature by employing a Forma-Temp Jr. Model 2095 thermostated bath. The cells were kept in the dark, and the room was also darkened while absorbance readings were being taken. For runs near ambient temperatures (21.1 and 31.1 °C), cells were kept in a water-filled beaker, which was removed from the bath when a reading was to be taken. The cell was removed from the beaker for only about 5 s while the absorbance value was being determined. The beaker and cell were out of the circulating bath for only about 15 s for each measurement; during that time, it was determined that the temperature within the beaker had changed by a negligible amount. Substrate concentrations of ca. 6×10^{-4} M and sufficient excesses of both py and L to maintain pseudo-first-order conditions in both reagents (in toluene solution) were employed. The decrease in absorbance of the substrate was monitored at 435 nm. Plots of ln ($A_t - A_\infty$) vs time (A_t and A_∞ are the absorbances at time t and at infinite time, >10 half-lives, respectively) were linear to at least 80% completion of the reaction. For some runs at 13.6 and 31.1 °C, conventional sampling techniques as described previously,[11] where the samples were quenched by cooling to 0 °C, were also employed; the rate constants obtained via the two methods were the same, within experimental error. Data were analyzed by employing a linear-least-squares computer program developed for our microcomputer. Values for the pseudo-first-order rate constants are presented in Appendix I (supplementary material). Error limits are given in parentheses as the uncertainty of the last digit(s) cited to 1 standard deviation.

Flash Photolysis Studies. Pulsed laser flash photolysis studies of reactions of (diphos)Mo(CO)$_4$ with py and various L and in the absence of py or L were carried out at the Center for Fast Kinetics Research, The University of Texas at Austin, employing a Q-switched Nd:YAG laser operating in the frequency-tripled mode at 355 nm (11-ns fwhi, 100-mJ maximum energy) as the photolysis source and a Xe lamp as the monitoring source. Other experimental details have been described else-

(7) For some representation examples of studies of catalysis employing photogenerated intermediates, see: (a) Wrighton, M. S.; Graff, J. L.; Kauslauskas, R. J.; Mitchener, J. E.; Reichel, C. L. *Pure Appl. Chem.* **1982**, *54*, 161. (b) Whetten, R. G.; Fu, K. J.; Grant, E. R. *J. Chem. Phys.* **1982**, *77*, 3769. (c) Whetten, R. G.; Fu, K. J.; Grant, E. R. *J. Am. Chem. Soc.* **1982**, *104*, 4270. (d) Weiller, B. H.; Lui, J.-P.; Grant, E. R. *J. Am. Chem. Soc.* **1985**, *107*, 1595. (e) Wuu, Y.-M.; Bentsen, J. G.; Brinkley, C. G.; Wrighton, M. S. *Inorg. Chem.* **1987**, *26*, 530.

(8) (a) Wadsworth, W. S., Jr.; Emmons, W. D. *J. Am. Chem. Soc.* **1962**, *84*, 610. (b) Heitsch, C. W.; Verkade, J. G. *Inorg. Chem.* **1962**, *1*, 392.

(9) Chatt, J.; Watson, H. R. *J. Chem. Soc.* **1961**, 4980.

(10) Dobson, G. R.; Houk, L. W. *Inorg. Chim. Acta* **1967**, *1*, 287.

(11) Dobson, G. R.; Faber, G. C. *Inorg. Chem.* **1968**, *7*, 584.

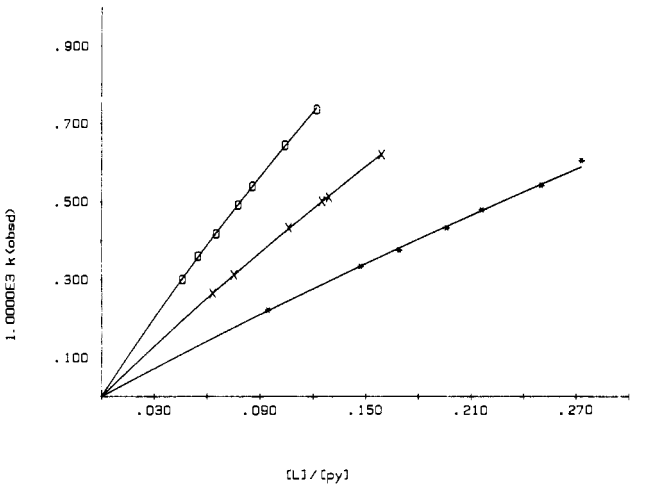

Figure 1. Plots of k_{obsd} vs [L]/[py] for reaction of *fac*-(py)(diphos)-$Mo(CO)_3$ with pyridine and L (○ = $P(OCH_2)_3CCH_3$; X = $P(OMe)_3$; * = $P(O\text{-}i\text{-}Pr)_3$) in toluene at 31.1 °C.

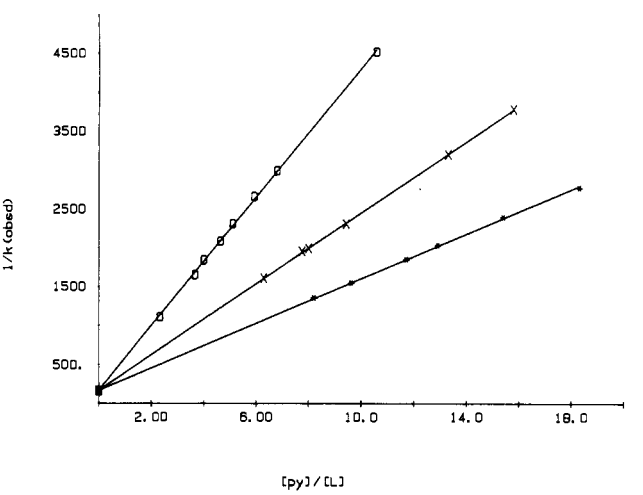

Figure 2. Plots of $1/k_{obsd}$ vs [py]/[L] for reaction of *fac*-(py)(diphos)-$Mo(CO)_3$ with pyridine and L (* = $P(OCH_2)_3CCH_3$; × = $P(OMe)_3$; ○ = $P(O\text{-}i\text{-}Pr)_3$) in toluene at 31.1 °C.

where.[4] Substrate concentrations of ca. 6×10^{-4} M in toluene were employed. For py, the wavelength monitored was 390 nm; for L and in the absence of py or L, it was 470 nm. Values of k_{obsd} are presented in Appendix II (supplementary material).

Results and Discussion

Mechanism of Ligand Exchange in *fac*-(py)(diphos)$Mo(CO)_3$. *fac*-(py)(diphos)$Mo(CO)_3$ produced photochemically through the reaction of (diphos)$Mo(CO)_4$ with py was identified as the fac isomer on the basis of its carbonyl stretching spectrum, which agrees with that reported for this complex as prepared thermally.[10] That spectrum is consistent with that expected for a molecule in which the C_{3v} local symmetry of the carbonyls is perturbed by the differing bonding properties of py and diphos. Thus the E mode in C_{3v} symmetry is split into A′ + A″ in C_s symmetry. E-mode splitting is also observed in the carbonyl stretching spectra for *fac*-(L)(diphos)$Mo(CO)_3$ products produced thermally through reaction of *fac*-(py)(diphos)$Mo(CO)_3$ with L (Table I). There was no evidence for the formation of reaction products that might result from the displacement of diphos, e.g., $(L)_2Mo(CO)_4$ species. The overall stoichiometry for the thermal reactions thus is

$$\textit{fac}\text{-(py)(diphos)}Mo(CO)_3 + L \rightarrow \textit{fac}\text{-(L)(diphos)}Mo(CO)_3 + py \quad (1)$$

Thermal kinetics studies were carried out, by and large, in the presence of "flooding" conditions of both py and L. Figure 1 shows representative plots of k_{obsd} vs [L]/[py] for reaction of *fac*-(py)(diphos)$Mo(CO)_3$ with large excesses of both py and L in toluene. They obey the rate law

$$k_{obsd} = k_a[L]/([py] + k_b[L]) \quad (2)$$

of a form that suggests a mechanism of successive steps, one or more of which is reversible. This expression can be rearranged to

$$1/k_{obsd} = [py]/k_a[L] + k_b/k_a \quad (3)$$

A mechanism shown in (4), to be discussed in greater detail later,

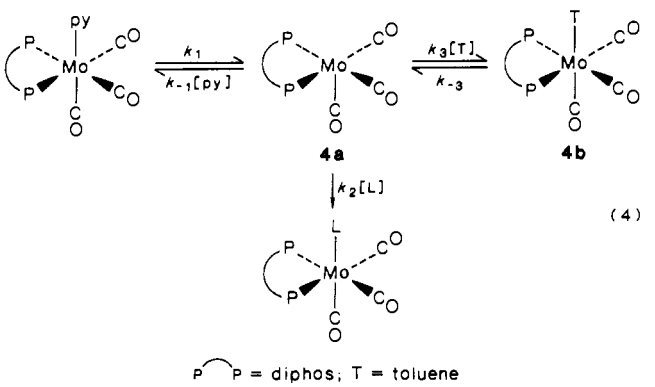

(4)

is consistent with these rate laws; this mechanism, which envisions initial Mo–py bond breaking, is analogous to that observed for ligand exchange in (diphos)$Mo(CO)_4$ with L, which takes place via rate-determining unimolecular fission of a facial Mo–CO bond.[11,12] Assuming steady-state concentrations of complexes **4a** and **4b**,[13] $k_a = k_1k_2/k_{-1}$ and $k_b/k_a = 1/k_1$. Since k_1 is independent of the identity of the incoming nucleophile, L, plots of $1/k_{obsd}$ vs [py]/[L] should have the same intercept for each L. This intercept, the value of [py]/[L] when [py] = 0, was determined both indirectly from these plots and directly through kinetics studies of ligand exchange in the presence of L but not py. Representative plots of $1/k_{obsd}$ vs [py]/[L], shown in Figure 2, demonstrate, as expected, that the plots for various L have a common intercept. From eq 3, in addition to values for k_1, can be extracted the "competition ratios" k_2/k_{-1} as intercept/slope. Values of k_1 and these competition ratios from data for six L are given in Table II, which also affords a comparison of values of k_1 obtained directly and indirectly via extrapolation of the plots of $1/k_{obsd}$ vs [py]/[L] to [py]/[L] = 0.

Table II. Rate Constants for Thermal Reactions of *fac*-(py)(diphos)$Mo(CO)_3$ with Pyridine (=Py) and L

L	T, °C	10^3k_1, s^{-1}		k_2/k_{-1}
$P(OCH_2)_3CCH_3$	31.1	6.2 (3)[a]	6.5 (5)[b]	1.06 (8)
$P(OMe)_3$		6.1 (3)	5.9 (8)	0.69 (6)
$P(OEt)_3$		6.15 (7)	5.9 (4)	0.58 (5)
$P(O\text{-}i\text{-}Pr)_3$[c]		6.2 (3)	5.9 (8)	0.41 (6)
	13.5	0.44 (1)		
	21.1	1.43 (4)		
PPh_3		5.99 (6)	6.2 (9)	0.44 (7)
$SbPh_3$	31.1	6.15 (9)	6.1 (4)	0.60 (4)

[a] Determined directly from kinetics runs employing no py. [b] Determined from intercepts of reciprocal plots (eq 3). [c] Activation parameters from values of k_1 at three temperatures: $\Delta H_1^* = 25.47$ (2) cal/(deg mol); $\Delta S_1^* = 16.05$ (6) cal/(deg mol).

Attempts were made to investigate ligand exchange for the still bulkier trio of ligands, $P(o\text{-tol})_xPh_{3-x}$ (x = 1–3). For L = P(*o*-tol)Ph_2, displacement of py at a rate approximating that observed for other L (via rate-determining dissociation of py) was observed; however, in the presence of both py and L, the reaction proceeded to an equilibrium mixture of *fac*-(py)(diphos)$Mo(CO)_3$ and the expected product. For L = $P(o\text{-tol})_2Ph$ and $P(o\text{-tol})_3$, some ev-

(12) Dobson, G. R.; Asali, K. J.; Marshall, J. L.; McDaniel, C. R., Jr. *J. Am. Chem. Soc.* **1977**, *99*, 8100.

(13) The mechanism shown in eq 4 presumes that desolvation takes place via a pathway involving rate-determining unimolecular dissociation of toluene rather than via an interchange process. This has been shown to be the case for solvent displacement (CB = solvent) from *cis*-[(CB)($P(O\text{-}i\text{-}Pr)_3$)$W(CO)_4$].[6]

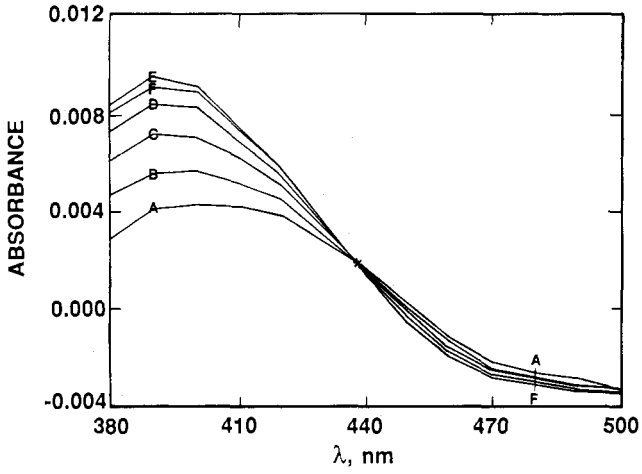

Figure 3. Time-resolved spectra after flash photolysis of (diphos)Mo(CO)$_4$ in pyridine/toluene solution (0.265 M) at 31.1 °C. Times after flash (μs): A, 0.28; B, 0.68; C, 1.28; D, 2.18; E, 3.38; F, 4.58.

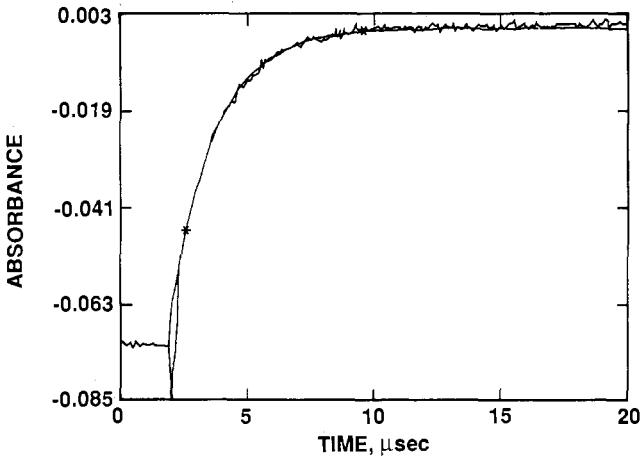

Figure 4. Plot of absorbance vs time for reaction with pyridine (0.0263 M) of the species produced after flash photolysis of (diphos)Mo(CO)$_4$ in toluene at 31.1 °C. The wavelength monitored was 390 nm.

idence for product formation was noted, but their reactions with *fac*-(py)(diphos)Mo(CO)$_3$ eventually led to the decomposition of the products to (diphos)Mo(CO)$_4$.

Mechanism of Reactions following Flash Photolysis of (diphos)Mo(CO)$_4$. Photolysis of a THF solution of (diphos)Mo(CO)$_4$ and subsequent addition of L affords *fac*-(L)(diphos)Mo(CO)$_3$ in high yield. This reaction

$$\text{(diphos)Mo(CO)}_4 \xrightarrow[\text{THF}]{h\nu} [\text{(THF)(diphos)Mo(CO)}_3] \xrightarrow[\text{fast}]{+\text{L}} \textit{fac}\text{-(L)(diphos)Mo(CO)}_3 \quad (5)$$

indicates that CO is lost upon photolysis of (diphos)Mo(CO)$_4$ with retention of geometry;[14] thus, the likely transient generated in toluene solution is *fac*-[(T)(diphos)Mo(CO)$_3$]; here again, no products attributable to loss of diphos were observed. Pulsed laser flash photolysis of (diphos)Mo(CO)$_4$ in the presence of excess py in toluene affords the time-resolved spectra illustrated in Figure 3. In this figure, absorbance is plotted vs wavelength with each trace taken at a different time delay after the flash; it indicates that the maximum change in absorbance occurs at about 390 nm. Similar plots for flash photolysis of (diphos)Mo(CO)$_4$ in the presence of various L (not illustrated) indicate that the best observation wavelength for reactions of L is 470 nm. Plots of A vs time, such as are shown in Figures 4 and 5 for photolysis in the presence of py and P(OCH$_2$)$_3$CCH$_3$, respectively, exhibited logarithmic decay or growth. From them were extracted the pseudo-first-order rate constants, k'_{obsd}.

(14) Rousche, J.-C.; Dobson, G. R. *Inorg. Chim. Acta* **1978**, *28*, L139.

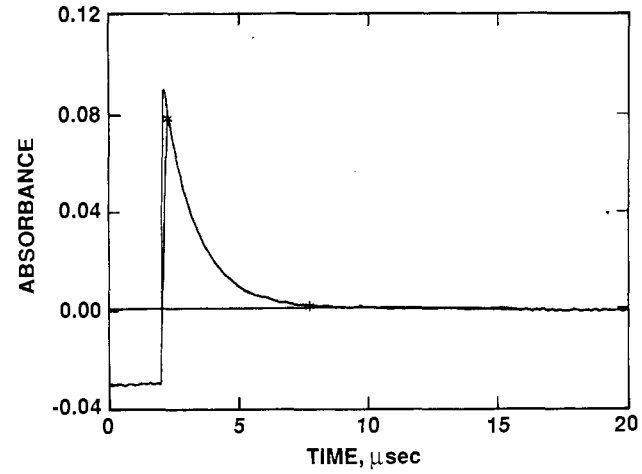

Figure 5. Plot of absorbance vs time for reaction with P(OCH$_2$)$_3$CCH$_3$ (0.0247 M) of the series produced after flash photolysis of (diphos)Mo(CO)$_4$ in toluene at 31.1 °C. The wavelength monitored was 470 nm.

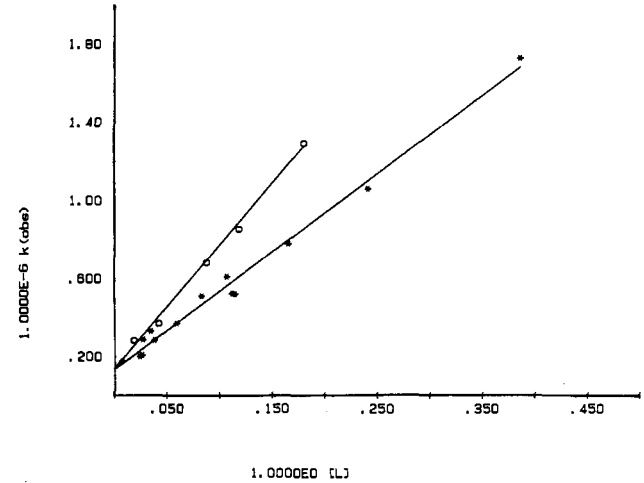

Figure 6. Plots of k_{obsd} vs [L] for reactions of L (○ = P(OEt)$_3$; * = P(O-*i*-Pr)$_3$) with the species produced after flash photolysis of (diphos)Mo(CO)$_4$ in toluene at 31.1 °C.

Table III. Rate Constants for Thermal Reactions with Pyridine and L after Flash Photolysis and Comparisons of Competition Ratios for Thermally and Photochemically Initiated Reactions Leading to Formation of *fac*-[(T)(diphos)Mo(CO)$_3$][a]

L	$10^{-6}k_{-1},k_2$, M^{-1} s^{-1}	k_2/k_{-1} thermal	k_2/k_{-1} photochem	$10^{-5}k_4$, s^{-1}
C_5H_5N	10.7 (5)			2.1 (4)
P(OCH$_2$)$_3$CCH$_3$	13.7 (4)	1.06 (8)	1.3 (1)	0.7 (2)
P(OMe)$_3$	6.2 (1)	0.69 (6)	0.58 (4)	2.06 (8)
P(OEt)$_3$	6.3 (2)	0.58 (5)	0.59 (5)	1.4 (2)
P(O-*i*-Pr)$_3$	4.0 (1)	0.41 (6)	0.37 (4)	1.3 (2)
PPh$_3$	4.5 (2)	0.44 (7)	0.42 (4)	1.3 (7)
SbPh$_3$	5.8 (8)	0.60 (4)	0.5 (1)	0.7 (6)

[a] All data obtained at 31.1 °C.

Values for k'_{obsd} as a function of [L] for six incoming L are presented in Appendix II (supplementary material).

The kinetics data obey the rate laws (6) and (7). Typical plots

$$k'_{obsd} = k_c + k_d[\text{py}] \quad (6)$$

$$k'_{obsd} = k_c + k_e[\text{L}] \quad (7)$$

of k'_{obsd} vs [L] are given in Figure 6. The intercepts of these plots, which are small and which thus have rather large error limits, but which, nonetheless, are real, indicate the presence of a competing unimolecular decay pathway.

The predominant and ligand-dependent reaction pathway is attributable to interaction of py and L with a reaction species produced after Mo–CO bond fission. Such an intermediate is

implicated as the photolytically generated species on the basis of the identity of the *fac*-(L)(diphos)$Mo(CO)_3$ products produced after CW photolysis. These products also are observed to be formed during the reactions of *fac*-(py)(diphos)$Mo(CO)_3$ with various L and, thus, must arise thermally from an intermediate produced through Mo–py bond fission. Comparisons of the competition ratios k_2/k_{-1}, independently derived from the thermal data for six L, and k_e/k_d, obtained from photochemical data, are exhibited in Table III. These comparisons show that the competition ratios determined thermally and photochemically are very similar, i.e., that $k_2/k_{-1} = k_e/k_d$, and thus implicate the same intermediate.

While the transient initially produced thermally and photochemically must be *fac*-[(diphos)$Mo(CO)_3$], the species present in predominant concentration after the flash and present during thermal ligand substitution as the steady-state intermediate in higher concentration is the solvated species, *fac*-[(T)(diphos)-$Mo(CO)_3$]. There has now been accumulated overwhelming evidence that coordinatively unsaturated species such as would be produced after photolytic bond fission undergo very rapid and specific solvation, processes that take place on the picosecond time scale; this evidence has in particular been developed for $[Cr(CO)_5]$, produced after flash photolysis of $Cr(CO)_6$.[15] Studies of *cis*-[(CB)(L)$W(CO)_4$] species in which the solvent is chlorobenzene (CB) have shown that solvent exchange with other nucleophiles (L) takes place via a solvation/desolvation equilibrium and that the energetics of solvent exchange are dominated by the strength of the metal–solvent bonding interaction.[6] The fact that solvation is so rapid, and consequently that the activation barrier to solvation (or to interaction of the intermediate with L) is extremely low, is consistent with this conclusion and further indicates that these coordinatively unsaturated species are geometrically quite similar to their solvated analogues.[6] Evidence thus implicates *fac*-[(T)(diphos)$Mo(CO)_3$] (**4b**) as the species produced in predominant concentration after photolysis and *fac*-[(diphos)$Mo(CO)_3$] (**4a**) as the species that reacts with L. If this is the case

$$k'_{obsd} = k_c + (k_{-3}k_{-1}/k_3[T])[py] \quad (8)$$

and

$$k'_{obsd} = k_c + (k_{-3}k_2/k_3[T])[L] \quad (9)$$

so that, on the basis of eq 6 and 7

$$k_2/k_{-1} = k_e/k_d \quad (10)$$

a conclusion consistent with the competition ratio data given in Table III.

The intercepts, k_c (eq 6 and 7), of the plots of k_{obsd} vs [py] or [L] (Figure 6; values, as k_4 (vide infra), are given in Table III) are small and thus exhibit rather large error limits. However, they are real, as is demonstrated by the decay observed after flash photolysis of (diphos)$Mo(CO)_4$ in toluene but in the *absence* of a "trapping" nucleophile. A typical plot of absorbance vs time for this process, fitted as an exponential decay, is shown in Figure 7. Values for these rate constants at several temperatures are given in Appendix III (supplementary material). At 31.1 °C it is 1.49 (8) × 10^5 s^{-1}, a value that falls nicely within the range of values observed for the intercepts of the plots affording rate laws 6 and 7, which average 1.4 (4) × 10^5 s^{-1}. Rate behavior such as exhibited in Figure 6 has been observed for a number of flash photolysis reactions involving chelate rings; the intercepts have been attributed to unimolecular ring closure after photolytically induced chelate ring opening,[4,5,16] and thus it is not unreasonable

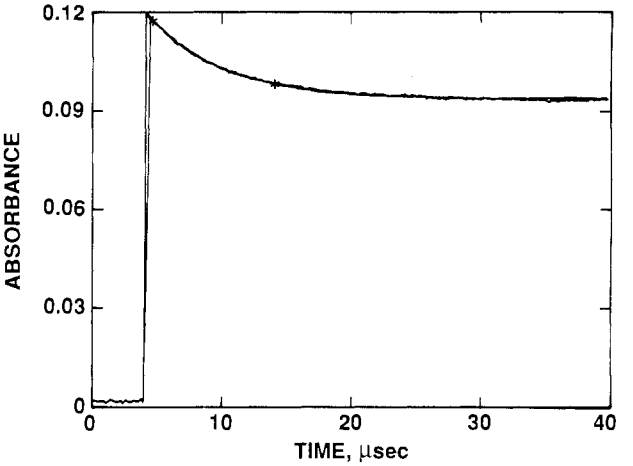

Figure 7. Plot of absorbance vs time for decay of the species produced after flash photolysis of (diphos)$Mo(CO)_4$ in the absence of L in toluene at 31.1 °C. The wavelength monitored was 470 nm.

to presume that it is a solvated[6] transient that decays via a ring closure, viz., *cis*-[(T)(η^1-diphos)$Mo(CO)_4$]. However, there is no evidence, either thermal[11,12] or photolytic, for the formation of a reaction product in which the chelate ring has been displaced from (diphos)$Mo(CO)_4$. Therefore, it may be concluded that this species decays exclusively via chelate ring closure to re-form the photolysis precursor, i.e., that ring reclosure is much faster than is attack by L at *fac*-[(η^1-diphos)$Mo(CO)_4$] in equilibrium with its solvated counterpart. This conclusion is reasonable in view of the activation parameters obtained for the unimolecular decay, $\Delta H^{\ddagger}$ = 7.7 (4) kcal/mol and $\Delta S^{\ddagger}$ = −9.3 (13) eu. This value for $\Delta S^{\ddagger}$ may be contrasted to that observed for solvent dissociation in *cis*-[(CB)($P(O\text{-}i\text{-}Pr)_3$)$W(CO)_4$], +5.6 (11) eu.[6] The negative entropy of activation for decay of the presumed *cis*-[(T)(η^1-diphos)$Mo(CO)_4$] intermediate suggests some bond making in the transition state leading to desolvation upon ring closure and that a potential solvent dissociation pathway, which also could afford the *fac*-(L)(η^1-diphos)$Mo(CO)_4$ product, is not competitive. Another possible attribution of the ligand-independent pathway, involving formation of a solvent-caged species after fission of the Mo–CO bond, which leads to formation of the observed *fac*-(L)(diphos)$Mo(CO)_3$ product, would not appear to be a reasonable alternative. The recombination of the caged fragments, for which the activation energy would be expected to be very small,[15] would be expected to take place on a much faster time scale than that monitored in these studies. Thus, the favored mechanism for thermal reactions following flash photolysis of (diphos)$Mo(CO)_4$ is that shown in eq 11.

Influence of Ligand Steric and Electronic Properties on the Rate of Ligand Exchange. Rates of solvent replacement from *fac*-[(T)(diphos)$M(CO)_3$] vary in the order $P(OCH)_2)_3CCH_3$ > py > $P(OMe)_3$ > $SbPh_3$ ≃ $P(OEt)_3$ > PPh_3 ≃ $P(O\text{-}i\text{-}Pr)_3$, an order which is neither that of increasing ligand size or decreasing ligand basicity, on the basis of Tolman cone angles and electronic parameters.[17] These observations suggest that both steric and electronic influences on reactivity are operative. In the sterically less demanding intermediates such as *cis*-[(CB)($P(O\text{-}i\text{-}Pr)_3$)$W(CO)_4$], rates of solvent displacement as a function of the steric and electronic nature of the incoming nucleophile, L, vary only about 2-fold;[6] thus, *fac*-[(T)(diphos)$Mo(CO)_3$], though appearing to be sterically more crowded, is no more discriminating among such nucleophiles. The crystal structure of (diphos)$Mo(CO)_4$ suggests that there should be surprisingly little steric congestion at the octahedral face containing diphos for ligands of moderate size;[18] this is quite evidently not the case for ligands such as

(15) (a) Welch, J. A.; Peters, K. S.; Vaida, V. *J. Phys. Chem.* **1982**, *86*, 1941. (b) Simon, J. D.; Peters, K. S. *Chem. Phys. Lett.* **1983**, *98*, 53. (c) Simon, J. D.; Xie, X. *J. Phys. Chem.* **1986**, *90*, 6715. (d) Langford, C. H.; Moralejo, C.; Sharma, D. K. *Inorg. Chim. Acta* **1987**, *126*, L11. (e) Simon, J. D.; Xie, X. *J. Phys. Chem.* **1987**, *91*, 5538.

(16) (a) Dobson, G. R.; Dobson, C. B.; Mansour, S. E. *Inorg. Chim. Acta* **1985**, *100*, L7. (b) Dobson, G. R.; Basson, S. S. *Inorg. Chim. Acta* **1986**, *105*, L17.

(17) Tolman, C. A. *Chem. Rev.* **1977**, *77*, 313.

(18) Bernal, I.; Reisner, G. M.; Dobson, G. R.; Dobson, C. B. *Inorg. Chim. Acta* **1986**, *121*, 199.

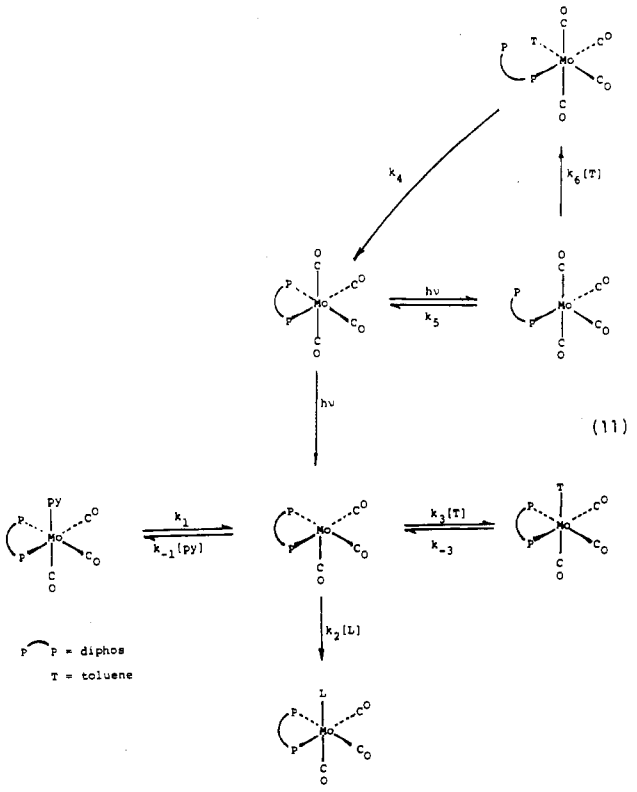

$P(o\text{-tol})_2Ph$ and $P(o\text{-tol})_3$ (vide supra); the latter has a cone angle of 190°.[17]

Nature of the Toluene–Mo Interaction. The strength of the solvent–metal interaction is the dominant influence upon reactivity in solvated intermediates of the group VIB metal carbonyls. For example, in *cis*-[(solvent)$(P(O\text{-}i\text{-}Pr)_3)W(CO)_4$] intermediates, rates of solvent displacement vary over 5 orders of magnitude from *n*-heptane (fastest) to bromobenzene (slowest)[6] and over a further 3 orders of magnitude in [(solvent)$Cr(CO)_5$] complexes for perfluoromethylcyclohexane (faster)[19] and cyclohexane[20] (slower) as solvents. Thus, the nature of the solvent–metal interactions in solvated intermediates such as *fac*-[(T)(diphos)$Mo(CO)_3$] produced upon flash photolysis is of great importance to the development of an understanding of their chemical reactivities. These interactions may be viewed as "normal" bonding interactions. In chlorobenzene solvent, for example, evidence has been presented that CB interacts with photogenerated group VIB metal carbonyl transients such as *cis*-[(L)$W(CO)_4$] through formation of a Cl-to-W coordinate bond; several complexes exhibiting RX-to-metal coordinate bonding are known,[21] and the infrared spectrum of a group VIB metal carbonyl complex containing coordinated dichloromethane has been reported.[22] Infrared spectral evidence in solution under ambient conditions indicates that [(*n*-heptane)$W(CO)_5$] and *cis*- and *trans*-[(*n*-heptane)(L)-$W(CO)_4$] are geometrically quite similar to their coordination complex counterparts such as (pip)$W(CO)_5$, *cis*-(pip)(L)$W(CO)_4$ (pip = piperidine), and *trans*-$(L)_2W(CO)_4$.[23] In these latter species, and in *fac*-[(T)(diphos)$Mo(CO)_3$] as well, the solvent-to-metal bonding interaction probably takes place through an "agostic" hydrogen,[24] that is, through formation of a three-center, two electron C–H–M bond. Extended Hückel calculations by Saillard and Hoffmann have shown that such an interaction of methane with coordinatively unsaturated [$Cr(CO)_5$] is "end-on",[25] from photoacoustic calorimetric results, its strength for *n*-heptane has recently been estimated to be ca. 10 kcal/mol.[26]

It is reasonable to view the interaction of toluene with Mo in *fac*-[(T)(diphos)$Mo(CO)_3$] as similar in nature, although evidence has also been presented which suggests that η^2-coordination of the arene might also be a viable bonding mode.[27]

The interaction of toluene with coordinatively unsaturated group VIB metal carbonyls is significantly stronger than is the analogous alkane–metal interaction. In this regard, it has been shown that the rate of solvent displacement from *cis*-[(solvent)(L)$W(CO)_4$] complexes by L, a rate that is predominantly influenced by the strength of the W–solvent interaction (vide supra), is some 65 times faster for *n*-heptane than for toluene.[6] It would appear unlikely, therefore, whatever the nature of the toluene–W interaction, that it takes place through the methyl group.

Acknowledgments. Support of this research by the Robert A. Welch Foundation (Grant No. B-434) and the National Science Foundation (Grant No. CHE 84-15153) is gratefully acknowledged. K.J.A. thanks the College of Education, King Saud University, Abha Branch, Abha, Saudi Arabia, for a sabbatical leave. G.J.v.Z. acknowledges the financial assistance of the University of the Orange Free State. The flash photolysis experiments and analyses of the data produced were carried out at the Center for Fast Kinetics Research (CFKR), The University of Texas at Austin. The CFKR is supported jointly by the Biotechnology Branch of the Division of Research Resources of the NIH (Grant No. RR00886) and by The University of Texas at Austin. The help and expertise of the staff at the CFKR are greatly appreciated.

Registry No. **1**, 19349-52-1; **4b**, 115889-94-6; C_5H_5N, 110-86-1; $P(OMe)_3$, 121-45-9; $P(OEt)_3$, 122-52-1; $P(O\text{-}i\text{-}Pr)_3$, 116-17-6; $P(OCH_2)_3CCH_3$, 1449-91-8; PPh_3, 603-35-0; $SbPh_3$, 603-36-1; (diphos)$Mo(CO)_4$, 15444-66-3; *fac*-$(P(OCH_2)_3CCH_3)$(diphos)$Mo(CO)_3$, 115889-91-3; *fac*-$(P(OMe)_3)$(diphos)$Mo(CO)_3$, 97202-30-7; *fac*-$(P(OEt)_3)$(diphos)$Mo(CO)_3$, 115940-58-4; *fac*-$(P(O\text{-}i\text{-}Pr)_3)$(diphos)$Mo(CO)_3$, 67265-36-5; *fac*-$(PPh_3)$(diphos)$Mo(CO)_3$, 115940-59-5; *fac*-$(P(o\text{-tol})Ph_2)$(diphos)$Mo(CO)_3$, 115889-92-4; *fac*-$(P\text{-}(o\text{-tol})_2Ph)$(diphos)$Mo(CO)_3$, 115889-93-5; *fac*-$(SbPh_3)$(diphos)$Mo(CO)_3$, 19349-54-3.

Supplementary Material Available: Appendixes I and II, consisting of tables of pseudo-first-order rate constants for thermal reactions of *fac*-(py)(diphos)$Mo(CO)_4$ and for photochemical reactions of (diphos)-$Mo(CO)_4$ with various L, respectively, and Appendix III, containing a table of pseudo-first-order rate constants at various temperatures for the ligand-independent pathway observed after flash photolysis of (diphos)-$Mo(CO)_4$ (8 pages). Ordering information is given on any current masthead page.

(19) Kelly, J. M.; Bonneau, R. *J. Am. Chem. Soc.* **1980**, *102*, 1220.
(20) Kelly, J. M.; Bent, D. V.; Hermann, H.; Schulte-Frohlinde, D.; Koerner von Gustorf, E. A. *J. Organomet. Chem.* **1974**, *69*, 259.
(21) (a) Lawson, D. N.; Osborn, J. A.; Wilkinson, G. *J. Chem. Soc. A* **1966**, 1733. (b) Crabtree, R. H.; Faller, J. W.; Mellea, M. F.; Quirk, J. M. *Organometallics* **1982**, *1*, 1361. (c) Uson, R.; Fornies, J.; Tomas, M.; Cotton, F. A.; Falvello, L. R. *J. Am. Chem. Soc.* **1984**, *106*, 2482. (d) Burk, M. J.; Crabtree, R. H.; Holt, E. M. *Organometallics* **1984**, *3*, 638. (e) Barcello, F. L.; Lahuerta, M. A.; Ubeda, M. A.; Foces-Foces, C.; Cano, F. H.; Martinez-Ripoll, M. *J. Chem. Soc., Chem. Commun.* **1985**, 43. (f) Solans, V.; Font-Altaba, M.; Aguilo, M.; Miratvilles, C.; Besteiro, J.; Lahuerta, P. *Acta Crystallogr., Sect. C: Cryst. Struct. Commun.* **1985**, *C41*, 841. (g) Cotton, F. A.; Lahuerta, P.; Sanau, M.; Schwotzer, W.; Solava, I. *Inorg. Chem.* **1986**, *25*, 3526.
(22) Beck, W.; Schloter, K. *Z. Naturforsch., B: Anorg. Chem., Org. Chem.* **1978**, *33B*, 1214.
(23) Dobson, G. R.; Hodges, P. M.; Poliakoff, M.; Turner, J. J.; Firth, S.; Asali, K. J. *J. Am. Chem. Soc.* **1987**, *109*, 4218.
(24) Brookhart, M.; Green, M. L. H. *J. Organomet. Chem.* **1983**, *250*, 395.
(25) Saillard, J.-Y.; Hoffmann, R. *J. Am. Chem. Soc.* **1984**, *106*, 2006.
(26) Yang, G. K.; Peters, K. S.; Vaida, V. *Chem. Phys. Lett.* **1985**, *125*, 566.
(27) Jones, W. D.; Feher, F. J. *J. Am. Chem. Soc.* **1984**, *106*, 1650.